I. J. Day
E. M. Greitzer[1]
N. A. Cumpsty

Whittle Laboratory,
University of Cambridge,
Cambridge, England

Prediction of Compressor Performance in Rotating Stall

A correlation is presented for predicting the performance characteristics of single and multistage axial compressors in rotating stall. The correlation is derived from new measurements of stalled compressor performance which have been obtained using a series of different compressor builds. In these experiments the compressor design parameters were systematically varied so that the influence of each could be clearly seen. It is shown that the stall cell blockage is an important parameter for correlating the flow regimes in stall, and hence the overall compressor performance. The resulting correlation, which has been developed based on a heuristic model of the stalled flow, can be applied to predict whether a given compressor will exhibit full-span or part-span stall, as well as the extent of the stall-unstall hysteresis loop. In particular, it is shown that as the number of stages and/or the design value of axial velocity parameter increases, the trend is toward both full-span stall and large hysteresis loops.

Introduction

When the flow rate through an axial compressor is reduced from the design value, the essentially steady, axisymmetric flow that exists becomes unstable. The result of this instability is very often manifested as a phenomenon known as rotating stall. In this flow regime one finds one or more regions of severely retarded flow rotating round the compressor annulus at a constant speed, which is commonly between 20 and 70 percent of rotor speed. The regions of retarded (or even reversed) flow are generally termed stall cells.

In many instances the consequences associated with the onset of rotating stall are quite severe. The flow rate and the delivery pressure can be markedly reduced, and the efficiency can also drop sharply. In addition there may be a large hysteresis between stall onset and cessation, which can seriously affect compression system recovery from stall. Further, there can be adverse effects on compressor blade life associated with the cyclic stresses generated by the stall cells, which subject both rotor and stator to a time-varying flow field. For these reasons, this phenomenon has come under considerable study in an attempt to isolate those factors which could lessen the possible unfavorable effects.

The first explanation of rotating stall was given by Emmons, et al. [1][2] almost 25 years ago. Since then, many other investigators have examined the problem both theoretically and experimentally and a useful bibliography is given in references [2, 3]. Almost all of the theoretical approaches, however, have been based on small perturbation analyses. While these are able to attack the question of the *inception* of rotating stall, the large flow nonuniformities that exist during the fully developed stages of rotating stall have not been successfully described by these theories. There have been some recent nonlinear numerical studies [4, 5] carried out, but these have so far been limited to an isolated rotor or a single stage and have provided mainly "qualitative clarification" [4] of some of the features of the stall cells. In addition, the analyses have been carried out under the restriction of a throttle with infinite impedance, i.e., a constant annulus average mass flow is maintained while the flow regime develops from unstalled to rotating stall. In practice the operating point of the compressor will be determined by the downstream throttle and, as the compressor delivery pressure drops during the transient from unstalled flow to fully stalled, the mass flow can also undergo a large amplitude transient.

Although there has also been a large amount of experimental work, this has generally examined such features of the phenomenon as number of stall cells and speed of propagation. Even with the extensive experimental effort, however, no clear pattern has emerged as to the physical parameters that control the basic features of the stalled flow. Furthermore, a detailed examination of the literature on rotating stall shows that there has been little effort on what would seem to be one of the primary goals as far as the compressor designer is concerned, namely, the prediction of the compressor characteristic in rotating stall, particularly for multistage compressors. Although some qualitative comments on these topics have appeared [6, 7] there has not been an attempt to establish a firm quantitative description. Specifically, one is interested in the influence of such design variables

[1] United Technologies Research Center, Silver Lane, East Hartford, Conn. This work was carried out while the author was on leave from Pratt & Whitney Aircraft.

[2] Numbers in brackets designate References at end of paper.

Contributed by the Gas Turbine Division and presented at the Gas Turbine Conference, Philadelphia, Pa., March 27-31, 1977, of THE AMERICAN SOCIETY OF MECHANICAL ENGINEERS. Manuscript received at ASME Headquarters December 7, 1976. Paper No. 77-GT-10.

as C_x/U, hub/tip ratio, number of stages, etc., on the performance in the rotating stall regime. This includes such quantities as the delivery pressure rise that one can expect during operation in rotating stall, and the size of the hysteresis between the point of onset and the point of cessation of rotating stall.

The present paper is focused on this aspect. The aim is to develop a framework upon which to build a systematic understanding of the influence of the physical parameters of a given axial compressor on the overall features of operation during rotating stall. It is clear from the outset that at present this cannot be done from "first principles" and the approach must be of a more empirical nature. Thus the material presented herein can be regarded as a correlative approach to the problem, using a series of experiments in which the design parameters were varied in order to examine the influence on the stall performance. The results of the tests, as well as of the other relevant data in the literature, have been used to develop a correlation which enables one to predict the basic features of the stalled performance curve. A crucial hypothesis in this, due to McKenzie [7], is that stalled compressors produce an approximately constant total-to-static pressure rise per stage, regardless of the details of the compressor design.

It should be stressed at the outset that the present work deals with stalled performance of compressors of moderate or high hub/tip radius ratio, with the lowest value of hub/tip ratio of any compressor used in the correlation being 0.6. In addition, the data have all been obtained in low-speed machines in which compressibility effects were not important. Further, the smallest "unit" that is considered in the correlation is the *stage* (inlet guide vane, rotor, stator), since, although isolated blade rows do have many qualitative features in common with single or multistage compressors, it is found experimentally that there can be significant quantitative differences between the behavior of the former and the latter.

The next section describes the general nature of the flow regimes that are encountered during stall and introduces the physical ideas that are the basis for the correlation. The experimental program is then outlined and the correlation presented. Finally, specific examples are given to show the applicability of the ideas for predicting the stalled flow performance of single and multistage compressors.

2 General Features of Rotating Stall in Axial Compressors

2.1 **Flow Regimes.** It is useful to describe the flow regimes encountered during compressor operation in rotating stall, and to relate this to the changes in compressor performance that can be expected. Let us consider a hypothetical compressor of, say, three stages, and examine the performance curves plotted in the form of ψ_{TS} versus ϕ, where ψ_{TS} = (exit static pressure − inlet total pressure)/ρU^2, and $\phi = C_x/U$. Two possibilities are shown in Figs. 1(*a*) and 1(*b*), which can be regarded as being composites of data examined by the authors. Fig. 1(*a*) shows a compressor whose performance curve is either continuous or has a small discontinuity in pressure rise (a few percent) at the stall limit point, *A*. (By the term "stall limit" we mean the point of inception of rotating stall or, equivalently, the point of instability of the axisymmetric flow in the compressor annulus.) This behavior, where

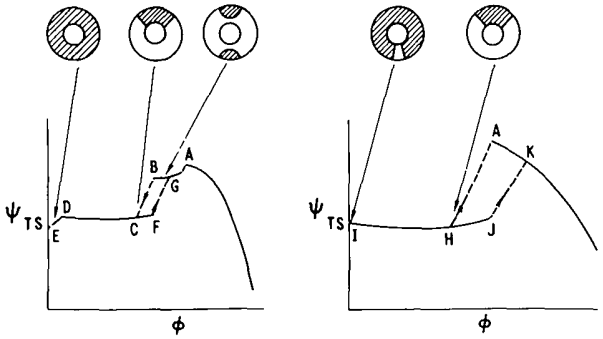

Fig. 1 Typical compressor characteristics

there is a very gradual drop in delivery pressure at the inception of stall, is associated with the compressor operating with one or more stall cells that do not cover the total height of the annulus. This is known as part-span stall, and an indication of a typical configuration is shown in the figure where we see two regions of severely retarded flow, i.e., two stall cells, at the tip. It is of course not always true that the cells appear at the tip; they can also be found at the hub, and the picture should just be regarded as giving one typical possibility.

As the throttle is closed from the stall point and the mass flow through the compressor illustrated in Fig. 1(*a*) is further decreased, the performance curve can exhibit a large discontinuity where the pressure rise and mass flow jump to significantly reduced values; this occurs from point *B* to *C* on the figure. This jump is associated with a change in the type of stall. At point *C* there is one single cell, occupying a sizable fraction of the annulus and extending over the full annulus height. This regime is known as full-span stall. Further throttling causes this cell to increase in size with the delivery pressure remaining relatively constant from point *C* to *D*. As the mass flow approaches zero, the stall cell can grow to fill the annulus so that the flow can become basically axisymmetric with the pressure rise often dropping off slightly. This would occur from *D* to *E*. If we were to once again open the throttle, we would find that the mass flow at which the compressor left the full-span stall regime, point *F*, was different from that at which it entered, although this hysteresis is usually negligible for the onset and cessation of part-span stall.

If we examine Fig. 1(*b*) we see a somewhat different picture. The large discontinuity in pressure rise and flow now occurs right at the stall limit (point *A*). The sharp drop in both these quantities as the operating point jumps from point *A* to point *H* is associated with the compressor going directly into single-cell, full-span stall, as indicated in the figure. Further throttling causes the stall cell area to grow, although it may not reach 100 percent of the annulus area even at zero mass flow through the compressor, with the pressure rise being relatively constant from point *H* to "shut off" at point *I*. If one opens the

Nomenclature

C_p = blade row loading parameter; = $\Delta p/q$ = $(p_{out} - p_{in})$/inlet dynamic pressure
C_p^* = C_p at design conditions
C_x = axial velocity
N = number of stages
p = static pressure
p_T = total pressure
U = mean rotor speed
α = flow angle relative to stators (measured from axial direction)
β = flow angle relative to rotors (measured from axial direction)
λ = stall cell blockage; represents the fraction of the compressor annulus occupied by fluid with zero through flow velocity
λ_{ps}, λ_{fs} = critical values of λ for part-span and full-span stall
ϕ = axial velocity parameter; $\phi = C_x/U$
ϕ^* = value of C_x/U at design conditions
$\bar{\phi}$ = annulus average axial velocity parameter
$\phi_{unstalled}$ (or ϕ_u) = axial velocity parameter at which unstalled region of compressor is operating
ρ = density
ψ_{TT} = nondimensionalized total pressure rise; $\psi_{TT} = [(p_T)_{exit} - (p_T)_{inlet}]/\rho U^2$
ψ_{TS} = nondimensionalized inlet-total to exit-static pressure rise; $\psi_{TS} = [p_{exit} - (p_T)_{inlet}]/\rho U^2$
Δp_{exit} = exit static pressure difference between stalled and unstalled regions

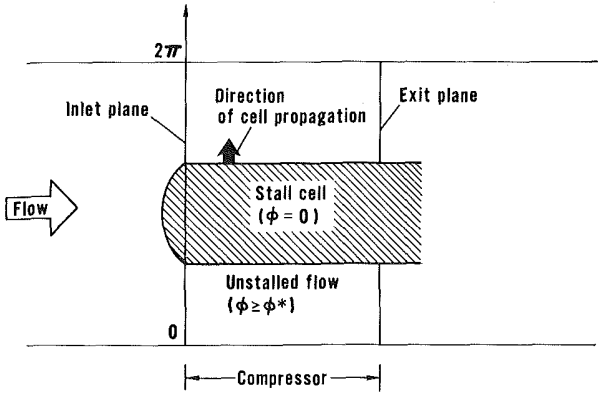

Fig. 2 Flow model for compressor performance in stall

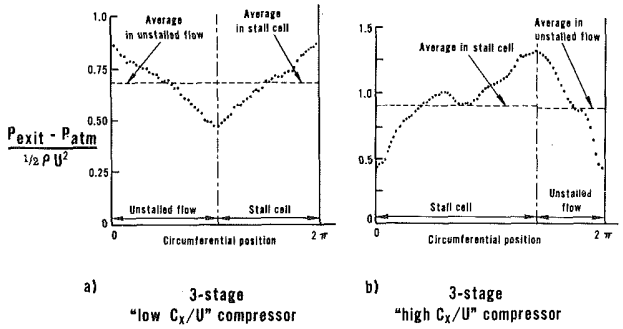

a) 3-stage "low C_x/U" compressor

b) 3-stage "high C_x/U" compressor

Fig. 3 Exit static pressure distributions

throttle it is again found that there is a substantial hysteresis between the onset and the cessation of stall.

The two types of behavior at the stall limit point shown in Figs. 1(*a*) and 1(*b*) have also been termed progressive and abrupt stall. This aptly describes the stall in terms of changes in the compressor output, since the former is associated with a relatively minor deterioration of the compressor performance from the unstalled state, but the latter can cause severe reductions in performance. However, it should be recognized that on a fluid mechanical basis the occurrence of these different types of behavior is due to operation in different modes of rotating stall. In order to predict the compressor performance subsequent to the onset of stall it is therefore important to be able to predict which type of rotating stall, part-span or full-span, will occur at the stall limit.

2.2 **Overall Flow Model.** In attempting to understand the relation between features of the stall cells and the performance parameters it is helpful to develop a basic model of the stalled flow. In doing this we take the simplest physically plausible hypothesis and view the flow in the compressor during rotating stall as consisting of a zone (or zones) of unstalled flow, in which the axial velocity is usually above the value corresponding to design conditions, and a zone (or zones) of stalled flow with zero axial velocity. In fact, the detailed measurements of Day [8] have shown that the net flow through the stall cell is not precisely zero although near enough to zero for it to be neglected in the heuristic model developed here. This description of the flow is illustrated in Fig. 2. The stall cell, which has zero axial velocity ($\phi = 0$) within it, is taken to extend axially through the compressor, this latter assumption also being strongly supported by the experimental results. It can be noted that even though the stall cell can be regarded as a region of zero net through flow, it is by no means a "dead" region (similar to the classical picture of a wake behind a bluff body, for example), as has been assumed by some authors. Despite the low *axial* velocity, the *circumferential* velocities in the cell can exceed blade speed in some cases. In addition, as described in [9], fluid is continually entering the stall cell from the unstalled region through the cell "trailing edge"[3] (the lower boundary of the cell in Fig. 2) and leaving through the "leading edge" so that the cell is a highly active region.

At the exit plane of the compressor we assume that both the stalled and unstalled regions have the same *average* static pressure. At first sight this may seem to be unwarranted, since with a traveling wave type of velocity distortion (such as a rotating stall cell) in a compressor the exit static pressure will not, in general, be constant [10]. However, the static pressure nonuniformities that occur in this situation will not be "in phase" with the velocity distortions. The maximum and minimum exit static pressures will commonly be found to occur on the boundaries of the stall cell. (A physical argument for this is given in [10].) Therefore the situation will be as illustrated in Fig. 3, which shows data from tests of two quite different three-stage compressors. The circumferential shift between the regions of "high" and "low" exit static pressure and the regions of high and low axial velocity (i.e., the regions of unstalled and stalled flow) means that the average exit static pressure in the unstalled flow and in the stall cell are very nearly equal. The degree to which this holds can be seen in the figure, which shows that the difference in average pressure in the two regions is indeed negligible. For a similar reason, the inlet total pressure variations at the compressor inlet, which occur due to unsteady flow effects, can also be neglected [8].

Thus, according to the model of rotating stall that we have adopted, the average pressure rise (inlet-total to exit-static) that occurs in the stall cell is equal to that in the unstalled region. However, we still cannot define the overall performance curve during operation in rotating stall, since we have not specified how this pressure rise will be determined. We must therefore consider in somewhat more detail the compressor pressure rise and flow during stalled operation.

2.3 **Flow and Pressure Rise in Stall.** As stated in the introduction, we cannot calculate the stalled flow performance of the compressor from first principles and must therefore develop the model using empirical information. Anticipating somewhat the experimental results that are discussed later, we introduce the hypothesis first proposed by McKenzie [7], that the nondimensionalized inlet-total to exit-static pressure rise ψ_{TS}, per stage, is a constant for compressors in part-span and in full-span stall, and that the magnitude of the pressure rise is more or less independent of the geometry of the compressor. Experimental results indicate that the constant total-to-static pressure rise is higher for operation in part-span than in full-span stall.

Some preliminary experimental support for this hypothesis, that the total-to-static pressure rise developed during stalled operation is independent of the design parameters of the particular compressor, is provided by the data of Yershov [11] who tested several different blade rows with quite different design parameters. His results are shown in Fig. 4, where it can be seen that the (unstalled) peak pressure rise differs by more than a factor of two for the various configurations, whereas the pressure rise in rotating stall shows considerably less variation. In particular, it should be noted that there appears to be no systematic dependence of stalled pressure rise on unstalled performance.

From the characteristic behavior of a stalled compressor it follows that for N stages the total-to-static rise is N times that for one stage, i.e., $\psi_{TS}(N) = N\psi_{TS}(1)$. It should be noted that since the pressure rise we are considering is the inlet-total to exit-static, this assumption implies a behavior that is fundamentally different from that in unstalled operation. Out of stall, if one examines the pressure rise for N identical stages, it is a reasonable approximation to say that both the total-to-total and static-to-static pressure rise for N stages are N times that for one stage. Thus if $\psi_{TT}(1)$ and $\psi_{TT}(N)$ are the non-

[3] This nomenclature, which is different from that used in [9], has been adopted to be consistent with the direction of propagation of the stall cell.

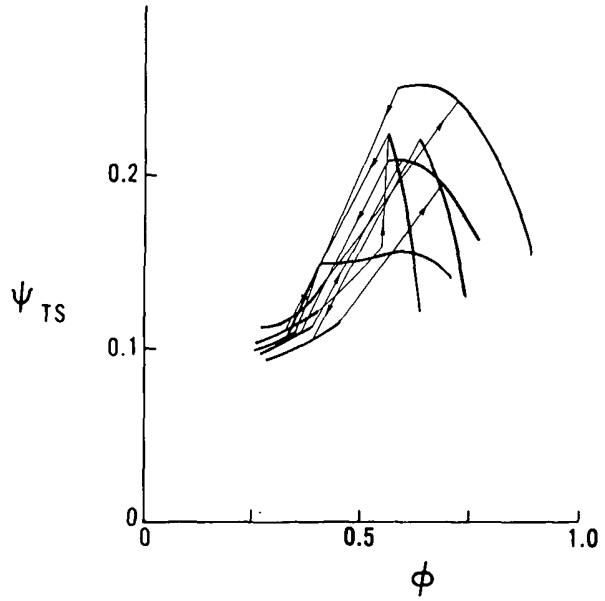

Fig. 4 Independence of stalled pressure rise and unstalled characteristic (after Yershov [11])

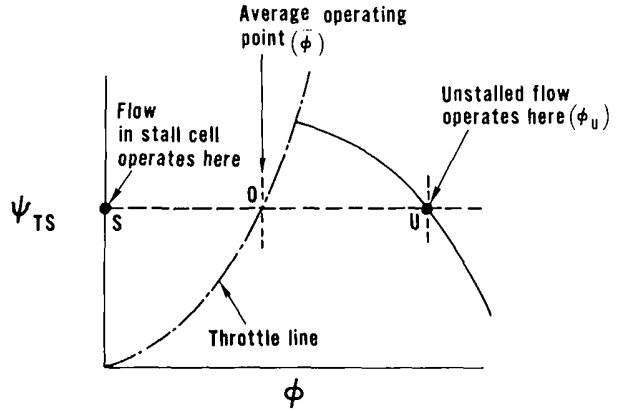

Fig. 5 Compressor operation in rotating stall

dimensionalized total-to-total pressure rises for one stage and N stages respectively, then

$$N\psi_{TT}(1) = \psi_{TT}(N) \tag{1}$$

The total-to-static pressure rise in unstalled flow for a single stage with an axial exit is given by

$$\psi_{TS}(1) = \psi_{TT}(1) - \tfrac{1}{2}\phi^2 \tag{2}$$

Similarly the total-to-static pressure rise in unstalled flow for N stages is

$$\psi_{TS}(N) = N\psi_{TT} - \tfrac{1}{2}\phi^2 \tag{3}$$

which is clearly not equal to N times the rise for one stage, since

$$N\psi_{TS}(1) = N\psi_{TT}(1) - \frac{N}{2}\phi^2 \tag{4}$$

Evidently the quantities on the left-hand sides of equations (3) and (4) are quite different and therefore the hypothesis that for *stalled* compressors $\psi_{TS}(N) = N\psi_{TS}(1)$ cannot be viewed as merely an obvious consequence of stacking stages together, but must be seen as reflecting a quite different flow model from that normally assumed for unstalled flow.

The idea that the nondimensionalized pressure rise per stage is a constant in the stalled regime has a further consequence when it is assumed that the total-to-static pressure rise is the same in the stall cell as in the unstalled region. This implies that as the compressor is throttled during operation in rotating stall, the "operating points" of each region do not change. Rather the fraction of the annulus that is operating in each type of flow changes, with the stalled part occupying more and more of the circumference as the throttle is closed, somewhat as sketched in the cell diagrams in Fig. 1.

Restricting, for the moment, our attention to full-span stall and again relying on empirical evidence that will be discussed later, it appears that the pressure rise in the stall cell is close to the overall total-to-static pressure rise of the compressor at the shut-off throttle setting (i.e., with zero net through flow). Thus, it is this shut-off pressure rise which determines the overall pressure rise delivered by a compressor in rotating stall. In the unstalled region the flow must therefore adjust itself so that this part of the compressor produces the same pressure rise, and this appears to be valid for both full-span and part-span stall. The detailed measurements reported in [8] show that in this unstalled part of the annulus the mass flow is approximately that associated with the specified pressure rise during steady operation. In other words, in the unstalled part of the annulus the compressor can be regarded as operating on the unstalled part of the steady-state characteristic at just the flow appropriate to the pressure rise set by the stall cell.

This situation is illustrated in Fig. 5, which shows the operating points, S and U, of the stalled and unstalled regions of the annulus, as well as the overall (annulus average) operating point 0. Since they both have the same inlet-total and exit-static pressure, S and U must be at the same value of ψ_{TS}. The annulus averaged flow, $\bar{\phi}$, is proportional to the net mass flow. It is determined by the throttle area and is related to the through flow in the unstalled region by

$$\bar{\phi} = (1 - \lambda)\phi_u \tag{5}$$

The overall (annulus averaged) operating point is thus at 0, with λ, the blockage of the stall cell, being defined as that fraction of the annulus that has no net through flow. According to this model as the throttle area is decreased the mean flow also decreases and λ thus approaches unity, reaching it at a zero mean flow.

Although the essential justification for this view of the stalled flow that we have adopted lies in experiment, one might also arrive at this picture using the following more intuitive argument. There appears to be no one salient point in the unstalled characteristic at which the compressor is any more likely to operate than any other. Consequently it should be expected that it is rather the stalled side, which is essentially operating at a condition corresponding to shut-off, that sets the level of pressure rise.

So far the model described is somewhat similar to those proposed by Gray [12] and McKenzie [7], although in the present case it has been bolstered by the detailed flow field measurements carried out during stalled operation. Up to this point we have not introduced information to allow us to decide whether full-span or part-span stall is likely, or to determine where the compressor unstalls. In order to do this we now postulate that there are critical values of the stall cell blockage. We infer from the data that there is a maximum blockage for part-span stall, λ_{ps}, and if the blockage exceeds this the compressor stall alters to full-span. We also infer that there is a *minimum* blockage for full-span stall, λ_{fs}, so that if the blockage falls below this critical value the compressor either unstalls or else changes to part-span stall.

2.4 **Prediction of Stalled Behavior.** These hypotheses for the stalled pressure rise and blockage conditions associated with the stall cells, coupled with the simple one-dimensional model that we have adopted of the flow in the compressor annulus, allow us to make predictions about the stalled characteristic. In particular it will be seen that they lead directly to a prediction of whether a compressor will operate in full-span or part-span stall, and to a quantitative prediction

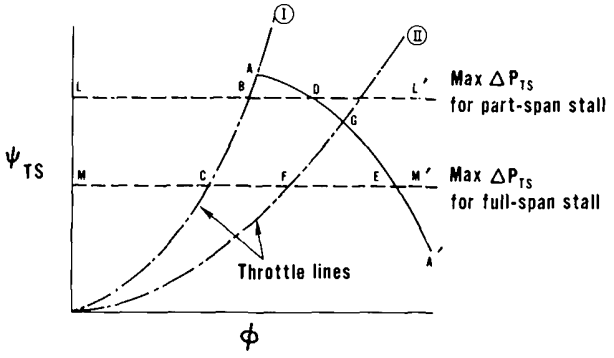

Fig. 6 Compressor performance in part-span and full-span stall

of the extent of the hysteresis region, both of which can be carried out from a knowledge of the unstalled part of the compressor curve only.

To illustrate more specifically the concepts that are involved, it is helpful to refer to Fig. 6, which shows a compressor characteristic with two throttle lines superimposed. One of these, line I, corresponds to the throttle setting at which the compressor flow becomes unstable, and intersects the unstalled part of the characteristic at point A. The other line, line II, corresponds to a somewhat larger throttle opening, specifically the throttle setting at the cessation of (full-span) rotating stall. Let us suppose that the only part of the compressor characteristic that is known is the unstalled part from A' to A, although the location of point G on this curve is unknown as yet.

In a conventional compressor test rig in which the compressor dumps into a relatively large plenum, which in turn exhausts to an exit throttle, the throttle curves will be parabolae through the origin. Therefore if the stall point is known the stall throttle line is also known, and so line I can also be assumed known.

The two horizontal lines LL' and MM' are the lines of operation at part-span and full-span stall, respectively, and intersect throttle line I at B and C. Our hypothetical model supposes that operation on the stall inception throttle setting (line I) is either at B (in part-span stall) or C (in full-span stall). To find out which it is, we visualize the compressor operating point as transiently moving down the throttle line with the blockage continually increasing. If the blockage at point B is less than the critical value for break down of part-span stall, λ_{ps}, the compressor will operate there in a part-span stall. If it is greater, it will drop to point C and operate there in full-span stall. Now from equation (5), the blockage, λ, is given by

$$\lambda = \frac{\phi_{\text{unstalled}} - \bar{\phi}}{\phi_{\text{unstalled}}} \tag{6}$$

Thus to find out whether part-span or full-span stall will be exhibited when stall first occurs, we need only find the ratio of the distance BD to LD, since the blockage, λ, is given by

$$\lambda = BD/LD, \tag{7a}$$

and compare this with the critical value, λ_{ps}.

In determining the extent of the stall/unstall hysteresis, we again make use of the concept of a critical blockage, λ_{fs}. Suppose now that the compressor represented by Fig. 6 is operating in full-span stall at point C. To return to unstalled operation from point C we increase the flow by opening the throttle. As this moves the operating point to the right along the line MM', the blockage will continually decrease. When the blockage has decreased past the critical value for operation in full-span stall, this mode is no longer possible, and the compressor undergoes a rapid transient to unstalled operation. This occurs at point F. At this point the blockage is equal to the ratio λ_{fs} so that

$$\lambda_{fs} = \frac{FE}{ME} \tag{7b}$$

which defines point F. Since we thus know the location of point F, and since the throttle lines are parabolae, the size of the hysteresis region is also determined, including point G at which the line II intersects the unstalled characteristic.

It is important to note that both the size of the hysteresis region and the determination of part-span or full-span stall are dependent on the shape of the throttle curve. This arises because the extent of the blockage, λ, depends on both compressor and throttle characteristics. Thus the mode of rotating stall depends not only on the details of the compressor blading but also on the properties of the entire compression system, since it is the demands of the throttling components that determine the mode of operation. This should be emphasized since, as mentioned in the introduction, some of the current analyses of rotating stall pose the problem with the annulus-averaged mass flow constrained to be constant during development of the cell. This is equivalent to imposing a throttle with infinite impedance, i.e., a vertical slope, and does not correspond to the conditions under which compressor testing is carried out. Since the throttle slope has an influence on whether operation is in the single cell or multicell regimes, some caution should be used in viewing the cell behavior that is calculated from these analyses.

The basic framework has now been sketched out upon which we will attempt to correlate the experimental results. It can be seen that the several hypotheses which have been made will, if verified, enable us to predict a great deal about the overall quantitative features of the stalled performance curve. We shall therefore now turn to the experimental examination of the assumptions used in the model.

3 Experimental Facility

The present study is based mainly on experimental work carried out in Cambridge on a 0.8 hub/tip radius ratio compressor which could be run with from one to four stages. Several sets of blades and vanes were available so that the stagger and camber could also be varied. Although the basic design was 50 percent reaction, the use of rotor and stator blades from the different sets enables the testing of different reactions as well. The compressor was driven by a constant-speed electric motor providing midspan rotor speed of 50 m/s, so that compressibility effects were not important. The compressor had both inlet and exit guide vanes, the latter being set so that the discharge was axial.

A schematic of the compressor in a typical (four-stage) configuration is shown in Fig. 7, where the measurement planes are also indicated. There were static pressure taps at the different locations to record the time averaged pressures. In addition, hot wires and pressure transducers enabled accurate measurement of the flow in the stall cell to be obtained. These latter measurements, which were carried out using a conditional sampling technique, have been reported elsewhere by Day [9] in some detail and will not be discussed except as they bear on the basic ideas of the present paper.

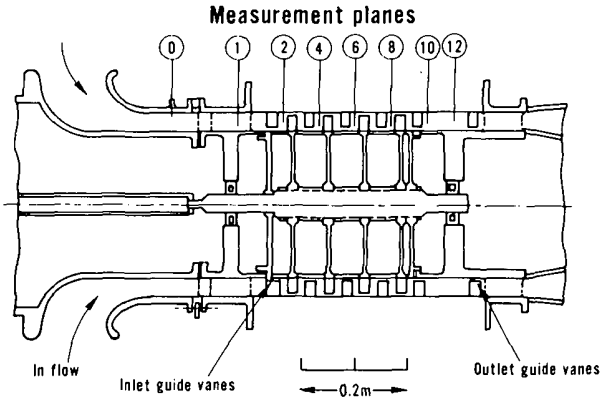

Fig. 7 Schematic of compressor showing four-stage build

Table 1 Design parameters of compressors used in correlation

COMPRESSOR BUILDS	NO. OF STAGES (N)	DESIGN C_x/U ($\approx \phi^2$)	DESIGN REACTION	STAGGER ANGLE (ROTOR/STATOR)	CAMBER ANGLE (ROTOR/STATOR	HUB/TIP RATIO
A (Low C_x/U)	1	.35	50%	50°/50°	20°/20°	.8
B (Low C_x/U)	3	.35	50%	50°/50°	20°/20°	.8
C(Intermediate C_x/U)	1	.55	50%	35°/35°	20°/20°	.8
D(Intermediate C_x/U)	2	.55	50%	35°/35°	20°/20°	.8
E(Intermediate C_x/U)	3	.55	50%	35°/35°	20°/20°	.8
F(Intermediate C_x/U)	4	.55	50%	35°/35°	20°/20°	.8
G (High reaction)	1	.71	65%	35°/20°	20°/40°	.8
H (High reaction)	2	.71	65%	35°/20°	20°/40°	.8
I (High reaction)	3	.71	65%	35°/20°	20°/40°	.8
J (High C_x/U)	1	1.00	50%	20°/20°	40°/40°	.8
K (High C_x/U)	2	1.00	50%	20°/20°	40°/40°	.8
L (High C_x/U)	3	1.00	50%	20°/20°	40°/40°	.8
M (High C_x/U)	4	1.00	50%	20°/20°	40°/40°	.8
OTHER COMPRESSORS						
N(Greitzer)	3	.65	45%	26.3°/30.4°	38.8°/10.1°	.7
O(Iura and Rannie)	3	.57	50%	43.9°/28.9°	20.2°/30.0°	.6

The experimental procedure was basically quite straightforward with a number of different types of compressors (i.e., builds with different blading, number of stages, etc.) being operated along a constant-speed line down to zero flow. Measurements were made of the overall compressor characteristic in the rotating stall regime, including the hysteresis between the onset of rotating stall when one closes the throttle and the cessation of stall when one opens it. During operation in rotating stall, fast response data were also taken in order to ascertain the type of stall (part-span or full-span) and the circumferential extent. The principal parameters of the different builds that were tested are given in Table 1, which lists the design values of C_x/U for each build, the number of stages, and the stagger and camber of the blades. It can be seen that the design parameters cover a reasonably wide range. The compressor characteristics from all the builds are given by Day [8].

It should be noted that one cannot rely upon conventional flow measuring instrumentation in the stalled flow regime. This is due to the fact that the pitot or pitot-static probes usually used for unstalled flow measurements in compressors are typically several chords upstream of the first blade row. When operating with full-span stall this means that these probes are imbedded within a highly nonuniform, unsteady flow, and large errors can result. As an example, in a recent compressor test by one of the authors (EMG) it was found that the conventional instrumentation was registering a flow that was roughly 30 percent of the design flow when the throttle was in a shut-off position. Therefore in the present series of experiments a calibrated orifice plate was used to provide the values of mass flow under stalled conditions.

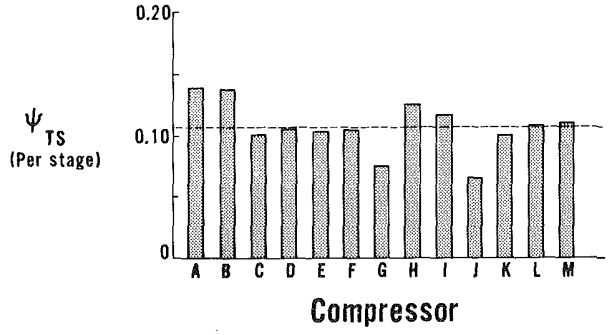

Fig. 8 Pressure rise per stage at shut-off for different compressors

4 Experimental Results

The most basic idea in the present model is that the nondimensional total-to-static pressure rise developed per stage during stalled operation is independent of the design parameters of the particular compressor. In addition, during operation in full-span stall the total-to-static pressure rise is equal to the pressure rise obtained during operation at the shut-off throttle condition. We have already seen some experimental justification of this in the single-stage data presented in Fig. 4. However, this hypothesis was examined much more fully in the present set of experiments. The results are presented in Fig. 8, which shows the nondimensional inlet total to exit static pressure rise *per stage* at the shut-off throttle condition for all the builds that were tested. The specific compressor configurations denoted by the letters on the abcissa of the figure are given in Table 1. It can be seen that the values are reasonably clustered about ψ_{TS} = 0.11 (absolute mean deviation less than 0.015). The larger departures from 0.11 are generally for the single-stage data (e.g., compressors *G* and *J*), with the multistage results having a smaller deviation from the mean.

Since the blockage at shut-off is such that full-span stall was always encountered, one cannot obtain information about the part-span stall pressure rise in the same manner. However, the data do indicate that the maximum total-to-static pressure rise measured during part-span stall was approximately constant and that a representative value is ψ_{TS} = 0.17 per stage [8]. This may be regarded as an upper value, for some compressors generate a peak unstalled pressure rise smaller than this, in which case the pressure rise in stall is approximately the same as that at stall inception. It is to be emphasized that the precise degree with which the assumptions are verified is held to be subsidiary to the general success of the correlation, as the eventual ability to predict will depend only on the latter. In any case the vagaries of stalled flow are such that agreement is to be regarded as satisfactory when it is less precise than is acceptable in unstalled flow.

The idea of a critical blockage can also be examined. In Fig. 9 the blockage is plotted for the different compressors in both part-span and full-span stall. The open points represent the *minimum* measured blockage found with full-span stall, and the solid points the *maximum* measured blockage that was attained with part-span stall. It can be seen that the minimum value for full-span stall, λ_{fs}, does not fall much below 30 percent, and similarly for part-span stall the maximum value, λ_{ps}, is always less than about 30 percent. There are insufficient data for the division to be made more precise than this at present, especially in view of the fact that there is generally a small flow through the stall cell, as mentioned earlier. It does seem that there may also be an influence of design C_x/U on the critical values, but this point cannot

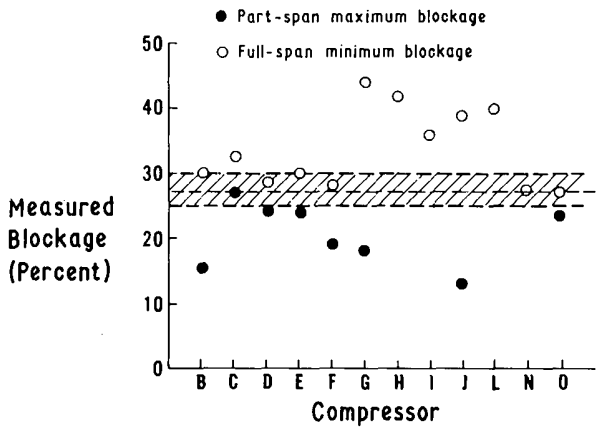

Fig. 9 Measured stall cell blockage for different compressors

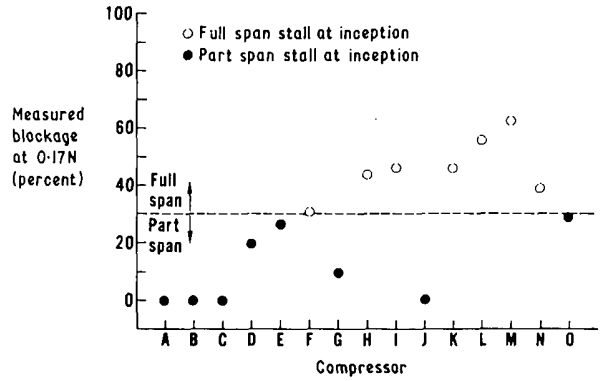

Fig. 10 Correlation of cell blockage for part-span or full-span stall at inception

be resolved without substantially more data. We therefore adopt (somewhat arbitrarily) that the upper limit of blockage for part-span stall and the lower limit of blockage for full-span stall should both be given by

$$\lambda_{ps} = \lambda_{fs} = 30 \text{ percent} \tag{8}$$

In the predictions carried out subsequently, then, rotating stall with blockage less than 30 percent will be assumed to be part-span and stall having blockages greater to be full-span. Moreover, a compressor operating in full-span stall for which the blockage is reduced (by opening the throttle) will either unstall or change to part-span stall if the blockage falls below 30 percent.

5 Stalled Performance Correlation

The results shown in the previous section are used here to provide a correlation of stalled flow performance. The specific aspects that have been examined are the question of whether a given compressor will exhibit part-span or full-span stall at the stall limit, and the extent of the hysteresis region. The model provides straightforward rules for answering these questions.

To determine whether the compressor will exhibit part-span or full-span stall at the instability point, we examine the stall-cell blockage that would exist at a pressure rise of $\psi_{TS} = 0.17N$. This, it may be recalled, is the typical maximum rise of an N-stage compressor in part-span stall. If the blockage is greater than 30 percent, full-span stall will occur; if less, part-span stall will occur. Stages which have an unstalled peak pressure rise of less than 0.17 per stage must be examined at their peak, where they have zero blockage, since 0.17 is a maximum value. The result of doing this using the measured, unstalled compressor characteristics and a parabolic throttle line through the measured stall inception point is shown in Fig. 10. This gives the blockage at $0.17N$, not only for all the compressors tested by Day, but also for two other three-stage compressors which are reported in the literature [13, 14]. It can be seen that the criterion that has been developed does indeed separate those compressors which encounter part-span stall from those in which full-span stall occurs.

The extent of the hysteresis in the stall and unstall behavior is also readily determined. The cessation of full-span stall as the throttle is opened is assumed to occur when the blockage has decreased to 30 percent. The value of the blockage is related to the ratio between the axial velocity in the unstalled part of the annulus and the annulus averaged axial velocity by equation (5). For 30 percent critical blockage, the ratio of the annulus averaged axial velocity to the axial velocity on the unstalled part of the characteristic curve (at a constant value of pressure rise of $0.11N$) is thus just

$$\frac{\bar{\phi}_{\text{cessation}}}{\phi_{\text{unstalled at } 0.11N}} = 0.70 \tag{9}$$

The measured values of this are plotted in Fig. 11 for the compressors tested, as well as for other results that can be found in the literature. It can be seen that the correlation is quite good, the points having a mean deviation from the predicted value of less than 7 percent.

Some comments should be made concerning the correlations shown in Figs. 10 and 11. First we can note that for the Iura and Rannie [13] compressor ψ_{TS} in part-span stall is somewhat higher than our tentatively adopted value of $0.17N$. Nevertheless, the correlation still correctly predicts the occurrence of part-span and full-span stall. It should also be noted that although data from the Iura and Rannie [13] and Greitzer [14] compressors were not used when formulating the "rules" for the correlation, the cessation point of full-span stall is correctly predicted in both cases. We regard the hypotheses, in particular the numerical values of the "constants," as prerequisites for the development of useful performance prediction criteria rather than precise statements in themselves.

6 Overall Performance Trends With Compressor Design

6.1 **Simple Analysis of Unstalled Performance.** The concepts that have been developed can be used to provide an understanding of the different trends that occur in stalled performance as certain compressor design parameters are changed. This is illustrated by carrying out a simple analysis of the unstalled performance of a compressor consisting of an inlet guide vane and N identical stages, in order to show the relation between the compressor design and the stall cell blockage. Since the aim is to present the topic in a manner which avoids unwarranted complexity, we will consider 50 percent

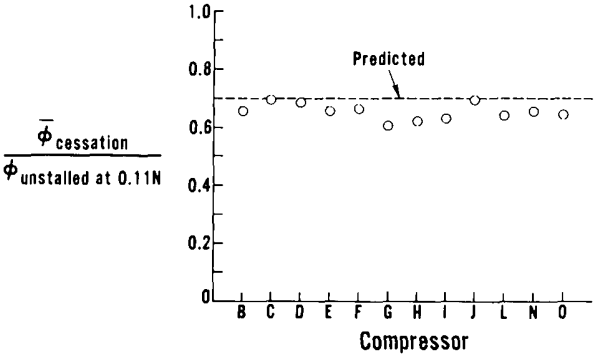

Fig. 11 Correlation for $\bar{\phi}$ at cessation of full-span stall

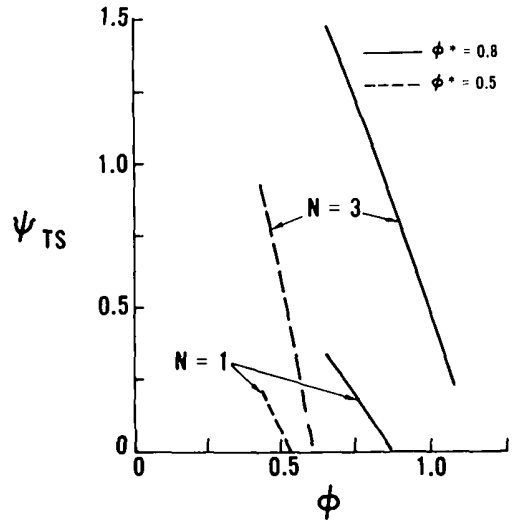

Fig. 12 Effect of number of stages, N, and design C_x/U, ϕ^*, on unstalled compressor characteristic

reaction stages having constant leaving angle and neglect losses over the unstalled flow range. These two idealizations do not change the basic nature of the results that are obtained, and a more complete model would merely alter the actual numerical values of the compressor performance curves slightly.

The family of compressors considered in this section all have the same design point loading, expressed here by the criterion of having the same value of $\Delta p/q$. This will be taken to be 0.4, which is a value representative of a conventional compressor in a gas turbine engine. We can also assume that the stall point will occur at a critical value of $\Delta p/q$, which is a given percentage higher than the design point value. Again, although this is somewhat of an idealization of existing empirical correlations for stall point, the adoption of a more complex criterion, such as those described in [15] or [16], for example, would not appreciably change the overall results. Specifically, therefore, we will say that the stall point is determined by

$$(\Delta p/q)_{\text{stall}} = 0.55$$

We can write the total-to-total (or static-to-static) pressure rise per stage as

$$\frac{p_{T3} - p_{T1}}{\rho U^2} = 1 - \frac{C_x}{U}(\tan\alpha_3 + \tan\beta_2) \tag{10a}$$

$$= 1 - 2\phi \tan\alpha_3 \tag{10b}$$

The subscript 1 refers to rotor leading edge, 2 to rotor trailing edge, and 3 to stator or inlet guide vane trailing edge, and $\beta_2 = \alpha_3$ since we are considering 50 percent reaction. The overall inlet-total to exit-static characteristic of an N stage compressor can thus be written:

$$\psi_{TS} = \frac{p_{\text{exit}} - (p_T)_{\text{inlet}}}{\rho U^2} = N[1 - 2\phi \tan\alpha_3] - \tfrac{1}{2}\phi^2 \sec^2\alpha_3 \tag{11}$$

Since we are examining the effect of design parameters (specifically number of stages and design C_x/U) on the performance of a family of compressors with the same design loading we must also derive a relation between ϕ^*, the design value of C_x/U, and the leaving angle α_3. This is obtained by combining the design loading criteria

$$C_p{}^* = (\Delta p/q)_{\text{design}} = 0.4$$

and the velocity triangle relationships to give a relation between the design flow coefficient, ϕ^*, the design pressure rise coefficient, $C_p{}^*$, and the exit flow angle, α_3. This is

$$\frac{1}{\phi^*} - \tan\alpha_3 = \frac{[C_p{}^* + (1 - C_p{}^*)\sin^2\alpha_3]^{1/2}}{\sqrt{1 - C_p{}^*}\cos\alpha_3} \tag{12}$$

Once ϕ^* is known in terms of α_3, equation (11) can be used to generate the idealized unstalled compressor curves, which are defined to the value of ϕ at which the stall value of $\Delta p/q$ is encountered.

To see the general trends that are implied by the design parameters, Fig. 12 presents four unstalled compressor characteristics. These are for one- and three-stage machines at values of ϕ^* equal to 0.5 and 0.8.

The important features to observe are that the peak total-to-static pressure rise of the machine for a given ϕ^* increases faster than proportional to N, that for a given number of stages the peak pressure rise increases with ϕ^*, and that the slope of the characteristic decreases as ϕ^* increases. Although Fig. 12 gives only isolated instances of these trends, calculations have been carried out for a range of values of ϕ^* and N, and the trends mentioned are well borne out.

6.2 **Stall Cell Blockage; Effect of ϕ^* and Number of Stages.** The analysis in the previous section points to the idea that the blockage (as defined in equation (5) and evaluated at a given level of ψ_{TS} equal to N times a constant value) will increase with both ϕ^* and number of stages. This can be seen more quantitatively in Fig. 13, which shows the stall cell blockage, evaluated at a value of ψ_{TS} equal to $0.11N$, for a range of compressors having different values of ϕ^* and number of stages. The throttle line used in defining the blockage is that corresponding to the stall inception point. Although the constant value 0.11 has been used, it should be noted that similar trends would occur at other physically plausible values.

The figure shows the blockage as a function of ϕ^*, for compressors having different numbers of stages. It is evident that for a given number of stages an increase in ϕ^* implies an increase in blockage. Conversely, for a given value of ϕ^*, increasing the number of stages will also result in increased blockage. The trend toward increased blockage with both ϕ^* and number of stages implies that the tendency would be to exhibit full-spans stall at stall inception the greater the number of stages and/or the higher the design value of C_x/U, ϕ^*. In addition, the greater the blockage on the inception throttle line, the larger the increase in annulus average mass flow that must occur to decrease the blockage to the critical value for cessation of full-span stall. Therefore the factors that increase blockage will also be expected to increase the size of the overall hysteresis loop associated with the stall/unstall process.

6.3 **Prediction of Stalled Compressor Behavior Using the Blockage Concept.** The simple analysis has enabled us to make quantitative predictions about the effect on the stalled performance

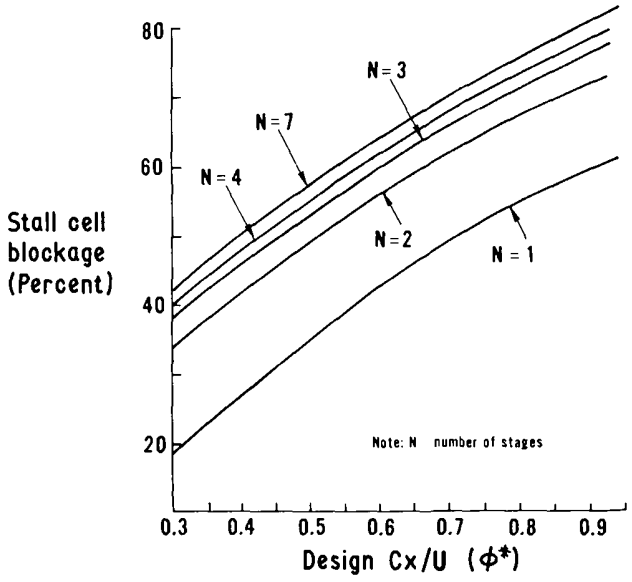

Fig. 13 Calculated values of stall cell blockage at $\psi_{TS} = 0.11N$ on the inception throttle line

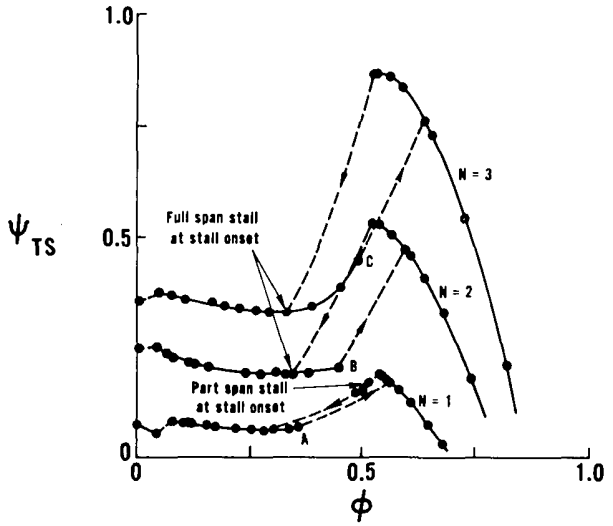

Fig. 14 Effect of number of stages, N, on stalled performance, $\phi^* = 0.55$

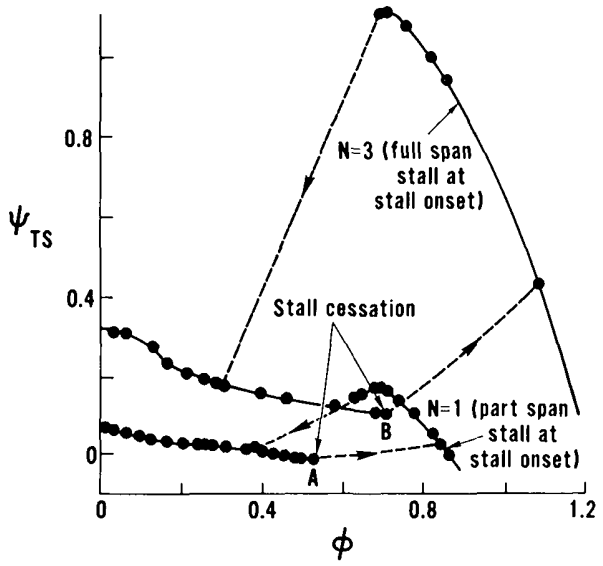

Fig. 15 Effect of number of stages, N, on stalled performance, $\phi^* = 1.0$

of different design variables. In particular we are able to show the effect of the number of stages and design flow, ϕ^*. We will now examine the applicability of these idealized concepts when used to predict the performance of actual compressors. In addition, we can also attempt to use the blockage concept to understand the transition from part-span to full-span stall exhibited by compressors having characteristic curves similar to the one shown in Fig. 1(a), and to point up the influence of throttle characteristic on the stalled performance.

Let us first consider the effect of number of stages. It has been noted by Yershov [11] and Day [8] that identical compressor stages will sometimes exhibit part-span stall when tested as a single stage, but will go into full-span stall when tested in a multistage configuration. The reason for this can be seen from the analysis. As N increases the ratio of peak unstalled total-to-static pressure rise to the constant pressure rise per stage in part-span stall will increase. Physically this is because the dynamic pressure at outlet becomes a smaller fraction of the overall pressure rise as N increases. Thus the blockage, which is proportional to the horizontal difference between the throttle line through the stall limit point (the value of ϕ at this point being the same, independent of N) and the unstalled part of the characteristic, will also increase. Thus, the larger the number of stages, the more likely the blockage will exceed the critical value and the more likely therefore to have full-span at inception.

This prediction is well illustrated by Fig. 14, which shows the measured compressor characteristics for configurations of one, two, and three identical stages. It can be seen that the peak pressure rise increases much more rapidly than N, and with it the blockage. In the three builds shown the blockages at a pressure rise of $0.17N$ are 10 percent, 36 percent, and 45 percent for the one, two, and three stages, respectively. Thus, according to the correlation, the single stage should exhibit part-span stall and the two- and three-stage machines full-span stall. The data indicate that this does indeed occur.

It is noteworthy that both these types of stall have been encountered with stages that have the same stagger, camber, gap/chord ratio, and most importantly hub/tip ratio. This last can be remarked since it has been implied by other authors that the division of compressors into those exhibiting part-span stall or full-span stall can be done on the basis of hub/tip ratio. From the data presented here it can be seen that this is not the case. Although it appears to be true that, in general, stages with low hub/tip radius ratio will exhibit part-span stall (possibly because the part of the blading that is stalled has quite a low blockage compared to total annulus area) the behavior of compressors of moderate or even high hub/tip radius ratio can be either part-span or full-span depending upon the blockage conditions.

Another aspect of the performance that can be seen in Fig. 14 is the size of the hysteresis loop. The simple analytical results indicate that the blockage at a value of $0.11N$ increases with number of stages for a given throttle setting, and also that the actual annulus averaged value of C_x/U that is required to achieve the critical blockage necessary for the cessation of full-span stall should increase with number of stages. This trend can be seen in Fig. 14 where the points at which full-span stall ceases (points A, B, and C for the one, two, and three-stage compressors) move to larger and larger values of C_x/U as N increases. A further illustration of this effect is given in Fig. 15, which shows an even larger increase in the size of the hysteresis loop as the number of stages is increased for compressors which have higher design flow rate.

The number of stages is thus one parameter that has been shown to have an effect on the nature of the stalled performance. Another important parameter is ϕ^*, because this has a very strong influence on the slope of the unstalled part of the characteristic. The analytical results show that as ϕ^* is increased the ratio of peak pressure to constant stalled pressure rise increases for compressors having a given number of stages. This is well confirmed by Fig. 16, which shows data from four different three-stage compressors, all of the same hub/tip ratio. The throttle lines at stall inception are also superimposed, and so too is a line at $\psi_{TS} = 0.33$ (i.e., $0.11N$, where N, the number of stages, is equal to 3). It can be seen that all of them have roughly the same shut-off pressure rise, although they have quite different values of the peak pressure rise. Since the criteria for part-span or full-span stall depends on the blockage, which is proportional to the horizontal distance from the inception throttle lines to the unstalled part of the characteristic, it is clear that higher ϕ^* compressors will have substantially greater blockages whatever the precise value of the constant stalled pressure rise per stage that is used.

From this it can be concluded that there will be a tendency for high ϕ^* compressors to exhibit full-span stall and low ϕ^* machines part-span stall. In agreement with this, it was found that the only one of the four compressor builds tested here that went into a part-span stall was the low ϕ^* machine, denoted by 1 in Fig. 16.

The influence of ϕ^* (the design value of C_x/U) on the hysteresis loop can also be discussed. In Fig. 16 the stall inception throttle lines are relatively close together, but the unstalled portion of the characteristics for the four compressors are quite different. Again, since the blockage is proportional to the horizontal distance between the two curves, it is evident that the throttle will have to be opened consid-

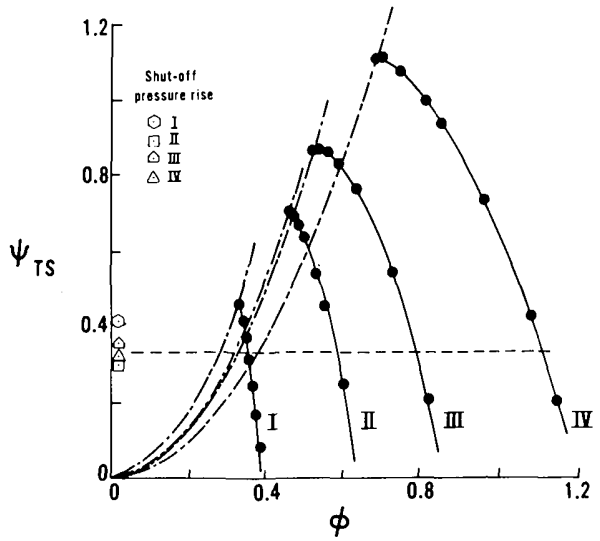

Fig. 16 Effect of design C_x/U, ϕ^*, on blockage (three-stage compressors)

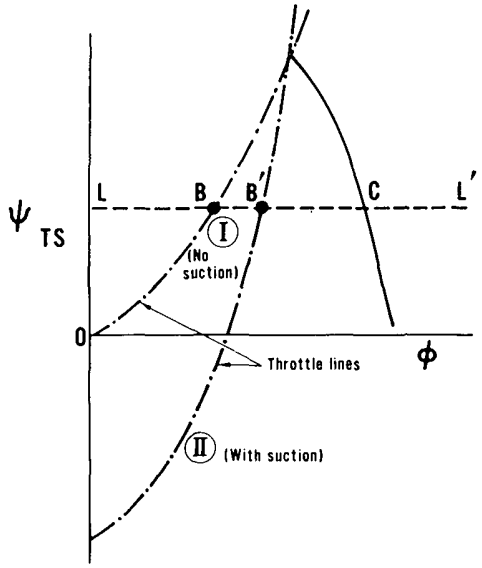

Fig. 18 Effect of throttle slope on stalled performance

erably further in the case of the high ϕ^* compressor (curve IV) in order to decrease the blockage to the critical 30 percent value for the cessation of full-span stall. The trend should consequently be toward larger hysteresis loops as ϕ^* increases. This can be seen in Fig. 17, which shows the measured characteristics of the different three-stage compressor builds that were tested. At the lowest value of ϕ^* (curve I) no hysteresis could be found. However, as we examine compressors with progressively higher values of ϕ^*, we find that there is an increase in the extent of hysteresis, just as the model would indicate. (The extent of hysteresis shown on the figure is the difference in ϕ between points on the stalled part of the characteristic corresponding to throttle settings at the inception and the cessation of stall.)

The stall model that has been developed and the general concepts that we have been using can also be applied to the question of the part-span/full-span transition that occurs in compressors having characteristics of the type represented by Fig. 1(*a*). We have concluded that the part-span stall does not exist if the total blockage is larger than 30 percent, and this can be used as a rough criterion for the transition from part-span to full-span stall. Suppose we have a compressor which exhibits a part-span rotating stall when it first

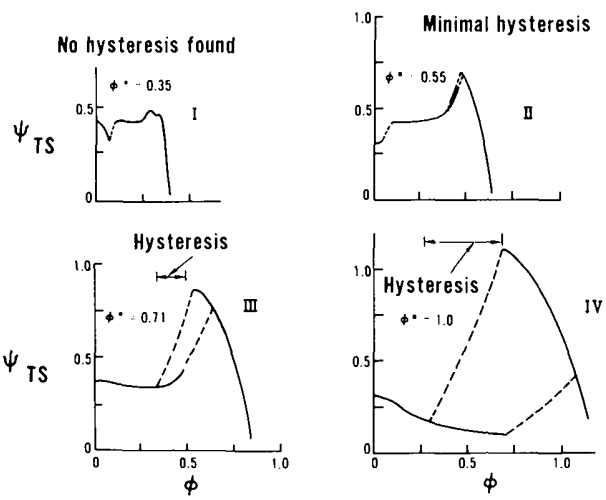

Fig. 17 Effect of design C_x/U, ϕ^*, on stall/unstall hysteresis (three-stage compressors)

stalls. Closing the throttle will cause the blockage to increase, until the critical value of 30 percent is reached, whereupon the flow regime changes to full-span stall. Although this prediction is not quantitatively precise, the trends of the data seen by the authors do indeed show this kind of behavior so that once again the model is able to provide some understanding of the overall compressor behavior.

As a further example of the usefulness of the concepts that have been developed, we can look at the influence of the throttle slope on the stalled performance. The basic ideas are sketched in Fig. 18. We see the one unstalled compressor characteristic with two different throttle lines going through the stall point. The line I corresponds to the usual case where the throttle curve is a parabola through the origin. Line II corresponds to the case where, for example, we have an exhauster or auxiliary compressor downstream of the throttle, so that the throttle is dumping to a pressure lower than atmospheric. In this case the curve will still be a parabola, but the parabola will cross the vertical axis somewhere below the point of zero pressure rise.

The important point to note in Fig. 18 is the difference in blockage that exists along any line of constant pressure rise, say line LL'. Since $BC > B'C$, the steeper the slope of the throttle line the smaller the blockage. Comparing two tests with the same compressor, one with the throttle dumping to atmosphere and the other using a downstream exhauster, one would therefore expect that the first would be more likely to exhibit full-span stall, because of the higher blockage dictated by the shallower throttle slope, while the second is more likely to show part-span stall. (Whether or not full-span or part-span stall occurs, depends also on the compressor characteristics, of course.)

This experiment could not be carried out with the present facility, but such a test has actually been performed by Borisov, et al. [17] using single-stage compressors of three different hub/tip ratios from 0.75 to 0.875. With the usual throttle exhausting to atmosphere there is a discontinuous characteristic at stall with one rotating stall cell, a behavior that we would associate with the onset of full-span stall. The use of suction behind the throttle valve, however, changes the characteristic into a continuous curve. The two different results are shown in Fig. 19. Although few details of the cell structure are given, one can only associate this gradual fall-off in efficiency and pressure rise with operation in part-span stall. The results of this experiment do support the arguments that the mode of stall that is obtained once the axisymmetric flow has become unstable does depend on the throttle conditions, and that for a stall model to give quantitative agreement

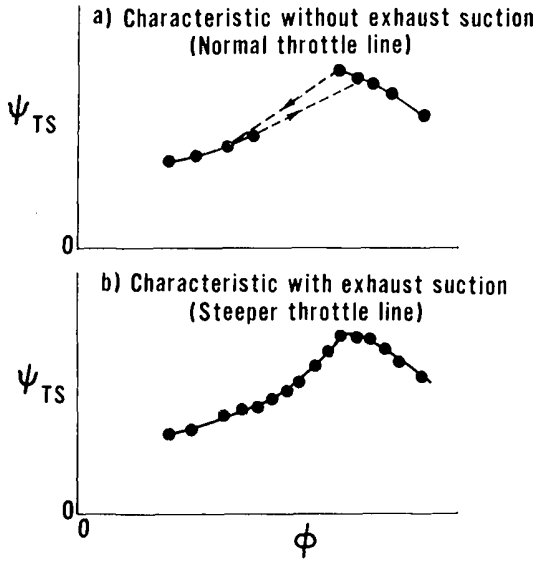

Fig. 19 Effect of throttle slope on stalled performance (after Borisov [17])

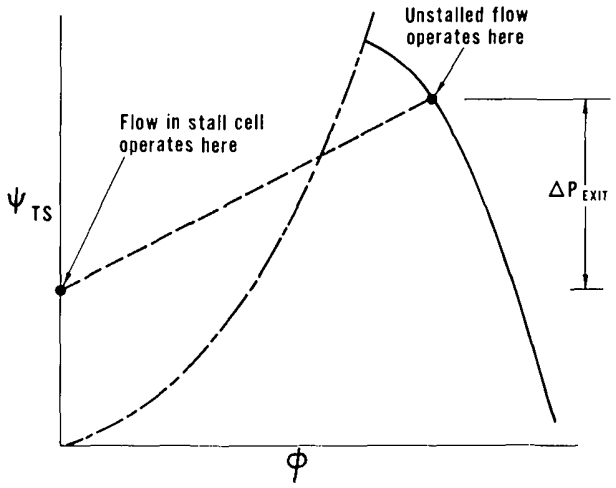

Fig. 21 Stalled compressor operation with nonuniform exit static pressure

with the experimental measurements, it may well be necessary to include the effects of the throttling system.

There is one further aspect of the experiments that we can also comment upon. This is the influence on stalled performance of downstream components. In order to explore this aspect, an experiment was conducted in which a screen (gauze) was placed close downstream of a three-stage compressor. The effect of the screen was such that the static pressure at exit of the compressor was no longer equal in the stalled and unstalled regions, due to the much higher pressure drop through the screen in the unstalled region. The unstalled region thus had a much higher exit-static pressure than the stalled region, as shown in Fig. 20. Under these conditions the stalled flow model would have to be modified to take this pressure drop into account, as shown schematically in Fig. 21.

The application of the model with the nonuniform pressure drop would imply that the overall performance curve would be sloping rather than flat, since the overall pressure rise can be regarded as the time average of the shut-off point and the operating point of the unstalled part of the flow. This conclusion is supported by Fig. 22, which shows the compressor performance curves with and without the screen. It can also be remarked that the screen has a strong influence on the axial velocity profile and tends to make the flow more uniform, i.e., to reduce the blockage. Thus the presence of the screen was responsible for the occurrence of a small flow regime in which part-span stall appeared in the compressor, whereas without the screen only full-span stall had occurred. This implies that in the stalled flow regime a downstream component could have a substantial effect on the compressor performance, in marked contrast to the situation in unstalled flow.

7 Suggestions for Future Work

It is to be emphasized that the authors regard the present correlation as a first step only in an attempt to provide an overall framework from which to view the complex and varied phenomena associated with rotating stall in axial compressors. As such, it seems appropriate here to present some suggestions concerning possible further work on this topic. One area of interest, of course, is the clarification of the fluid dynamic reasons for the nearly constant values of the nondi-

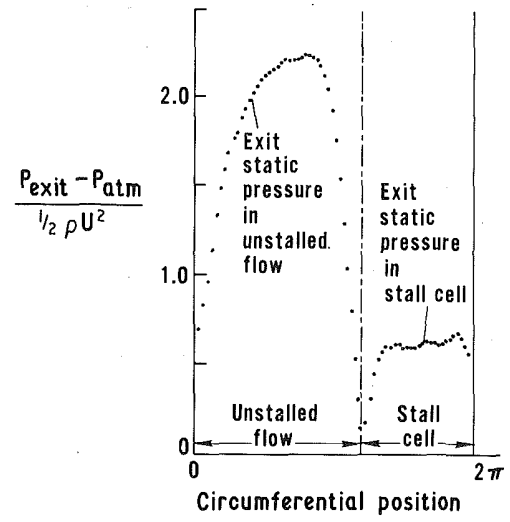

Fig. 20 Nonuniform exit static pressure induced by exit screen

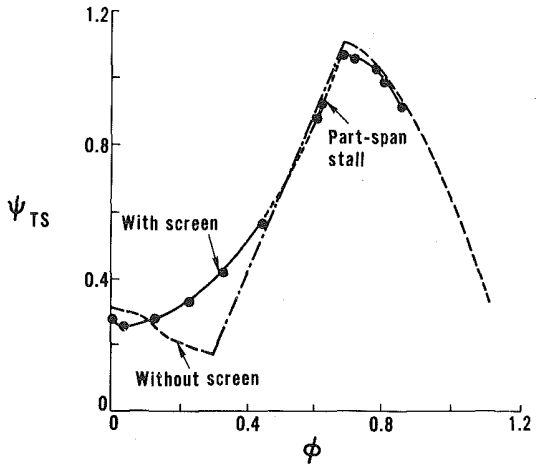

Fig. 22 Effect of exit screen on stalled performance

mensional stall pressure rise per stage and critical blockage. At present there is a lack of understanding about what sets the magnitude of these parameters, and analytical work in this area would be quite useful.

In addition, one of the limitations of the present study is that we were somewhat restricted in the parameters whose effects we could examine. There is thus a definite need for further parametric experiments. For example, the present range of applicability of the correlation is to compressors of moderate or high hub/tip radius ratio. However, if it were desired to extend the work to include stages of lower hub/tip ratio, it would be expected that hub/tip ratio would be a parameter that could have an effect on the flow regime encountered in rotating stall. For low hub/tip ratio compressors, which have very different local compressor characteristics, one might suspect that just the mean value of C_x/U would not be enough to totally describe the compressor behavior.

There are also several other parameters that might have an influence. For example, the experimental evidence on the structure of the stall cell points to a picture of the flow in which slow-moving air enters the rotor blades and is spun up to nearly blade speed before leaving the rotor, under the influence of centrifugal forces, and entering the stator blades where rapid irreversible deceleration occurs. The rotors and stators are thus acting roughly like fluid couplings, and one therefore suspects that the transference of momentum between rotating and stationary rows would depend on gross geometrical parameters such as solidity and aspect ratio (or passage aspect ratio). Although within the present data no such trends could be discerned, this may not be the case if one varies these parameters over more substantial ranges.

8 Summary and Conclusions

1 A model has been developed of the stalled flow in an axial flow compressor. The approach taken is to view the compressor as two separate compressors, one operating at zero flow and one at an axial velocity generally higher than the design value.

2 It is found that the blockage associated with the stalled region is an important parameter for correlating stalled performance.

3 Based on experimental evidence, four hypotheses have been adopted concerning the stalled performance:

(i) The total-to-static pressure rise per stage of a stalled compressor is largely independent of the compressor design. In full-span stall the nondimensional total-to-static pressure rise is approximately 0.11 per stage for all machines examined.

(ii) There is a critical value of stall cell blockage of 30 percent, above which part-span stall breaks down into full-span stall and below which full-span stall either changes to part-span stall or else collapses into unstalled flow.

(iii) The onset of part-span or full-span stall may be determined by the blockage at a nondimensional pressure rise of 0.17 per stage.

(iv) The flow rate at which the cessation of full-span stall occurs is determined when the blockage at a nondimensional pressure rise of 0.11 per stage drops to the critical value.

4 The use of these hypotheses in conjunction with the stall model enables one to correlate data from single and multistage compressors of moderate and high hub/tip ratio, and to formulate general predictive guidelines for the influence of design parameters on rotating stall performance.

5 For a given design value of C_x/U, the larger the number of stages in a compressor, the greater the chance of encountering full-span stall at the stall point, and the larger the size of the stall/unstall hysteresis loop.

6 For a given number of stages, the higher the design value of C_x/U, the greater the chance of encountering full-span stall at the stall point, and the larger the size of the stall/unstall hysteresis loop.

7 The slope of the compression system throttle line can have a significant influence on the stalled performance of the compressor, contrary to what has been assumed in most theories of stalled flow in axial compressors.

Acknowledgments

The authors would like to express their appreciation to Professor J. H. Horlock, Vice-Chancellor, Salford University, who, as well as giving initial impetus for this work, also provided guidance during the course of it. In addition, they wish to thank the Derby College of Arts and Technology for the loan of the test compressor and the British Ministry of Defence, Procurement Executive, for supporting the work. They are also grateful for the critical comments of Messrs. R. S. Mazzawy and J. P. Nikkanen of Pratt & Whitney Aircraft.

References

1 Emmons, H. W., Pearson, C. E., and Grant, H. P., "Compressor Surge and Stall Propagation," TRANS. ASME, Vol. 77, Apr. 1955, pp. 455–469.

2 Stenning, A. H., "Rotating Stall and Surge," Chapter 15, *ASME Lecture Course in Fluid Dynamics of Turbomachinery*, Iowa State University, Aug. 1973.

3 Fabri, J., "Rotating Stall in Axial Compressors," *Internal Aerodynamics (Turbomachinery)*, Institution of Mechanical Engineers, 1970 (also available as NASA Technical Translation TT F-11, 765, 1969 or ONERA Communication TP No. 492, 1967).

4 Takata, H., and Nagano, S., "Nonlinear Analysis of Rotating Stall," ASME Paper No. 72-GT-3, 1972.

5 Adamczyk, J. J., "Unsteady Fluid Dynamic Response of an Isolated Rotor With Distorted Inflow," AIAA Paper No. 74-49, Jan. 1974.

6 Dunham, J., "Asymmetric Flows in Axial Compressors," Mechanical Engineering Sciences, Monograph No. 3., Institution of Mechanical Engineers, 1965.

7 McKenzie, A., Private communication.

8 Day, I. J., "Axial Compressor Stall," PhD dissertation, Cambridge University Engineering Department, 1976.

9 Day, I. J., "Detailed Flow Measurements During Deep Stall in Axial Flow Compressors," *AGARD Conference Proceedings 177, Unsteady Phenomena in Turbomachinery*, 1976.

10 Greitzer, E. M., "A Note on Compressor Exit Static Pressure Maldistribution in Asymmetric Flow," Cambridge University Engineering Department Report CUED/A-Turbo/TR 79, 1976.

11 Yershov, V. N., "Unstable Conditions of Turbodynamics, Rotating Stall," U.S. Air Force Foreign Technology Division Translation FTD-MT-24-04-71, 1971.

12 Gray, S., Private communication.

13 Iura, T., and Rannie, W. D., "Experimental Investigation of Rotating Stall," TRANS. ASME, Vol. 76, Apr. 1954, pp. 463–471.

14 Greitzer, E. M., "Surge and Rotating Stall in Axial Compressors: Part II Experimental Results and Comparison With Theory," JOURNAL OF ENGINEERING FOR POWER, TRANS. ASME, Series A, Vol. 98, Apr. 1976, pp. 199–217.

15 Horlock, J. H., "Two-Dimensional Cascades: Experimental Work," Chapter 3, *Axial Flow Compressors*, Butterworths, London, 1958.

16 Leiblein, S., "Loss and Stall Analysis of Compressor Cascades," *Journal of Basic Engineering*, TRANS. ASME, Vol. 81, Sept. 1959, pp. 387–400.

17 Borisov, G. A., Lokshtanov, Ye. A., Ol'shteyn, L. Ye., "Causes of Break of Characteristics of Axial Compressor Stage with Large Relative Hub Diameter," *Blade Machines and Jet Devices*, U.S. Air Force Foreign Technology Division Translation FTD-MT-24-69-68, 1968.